International Journal of GEOMATE, June, 2025 Vol.28, Issue 130, pp.104-111
ISSN: 2186-2982 (P), 2186-2990 (O), Japan, DOI: https://doi.org/10.21660/2025.130.4938
Geotechnique, Construction Materials and Environment

FORCE-BASED METHOD FOR NONLINEAR ANALYSES OF CONTINUOUS STEEL-CONCRETE COMPOSITE GIRDERS

Hieu Nghia Hoang[1], *Quoc Anh Vu[2] and Manh Hien Nghiem[2]

[1]Department of Construction Engineering, Haiphong University, Vietnam; [2]Department of Civil Engineering, Hanoi Architectural University, Vietnam

*Corresponding Author, Received: 10 March 2025, Revised: 27 April 2025, Accepted: 28 April 2025

ABSTRACT: This study introduces an analytical approach for the nonlinear analysis of continuous steel-concrete composite girders. The proposed method achieves high accuracy by addressing key nonlinear effects, such as gradual and distributed yielding, while overcoming the limitations of conventional numerical techniques that rely heavily on element subdivision and complex computations. By utilizing three-moment equations from the force-based method, the approach establishes relationships between bending moments at three consecutive supports, enhancing the analysis of continuous girders and effectively capturing nonlinear flexural behavior. It should be noted that the method assumes full composite action and neglects shear slip effects, making it most suitable for flexure-dominated scenarios with adequate shear connection. The method's validity is confirmed through comparisons with advanced numerical simulations and full-scale experimental data from existing literature, demonstrating excellent agreement. These results establish the proposed approach as a dependable benchmark for validating numerical models and provide engineers with a practical yet precise tool for evaluating capacities and deflections of continuous girders.

Keywords: Continuous girders, Steel-concrete composite, Force-based method, Moment-curvature, Nonlinear analysis

1. INTRODUCTION

Researchers have proposed advanced methods for the analysis, design, and construction of bridge girders to ensure their safety throughout their service life [1,2]. Steel-concrete composite sections are widely used as composite beams in buildings and as composite girders in bridges, taking advantage of the combined material strengths of structural steel and concrete. Continuous girders offer additional benefits over simply supported girders, such as reduced deflection and redistribution of shear forces and bending moments. However, the design and analysis of continuous composite girders are more complex due to the differing behaviors in the positive and negative moment regions [3-5].

Three types of nonlinear analysis models for steel-concrete composite frames were proposed in the previous studies 1) Detailed finite element model: Developed using shell and solid elements; 2) Mixed finite-element model: A combination of beam and shell elements; and 3) Beam finite element model: Simplified representation using beam elements.

Detailed finite element models utilize shell elements for the flanges and webs of steel beams, along with shell or solid elements for reinforced concrete (RC) slabs [6-8]. These models effectively capture nonlinear material behavior and the slip effect between steel and concrete, making them valuable for analyzing local effects. However, their complexity and high computational cost make large-scale global analyses of steel-concrete composite girders challenging and often impractical. To balance accuracy and computational efficiency, mixed finite element models combining beam and shell elements have been proposed [9]. Zhou et al. [10] applied this approach for elasto-plastic numerical simulations of composite frames, while Vasdravellis et al. [4] used shell elements for the RC slab, beam elements for the steel beam, and spring or interface elements to model shear connectors. Nie et al. [9] also proposed a mix finite element model combining the fibered beam and layered shell elements using the general finite-element program. These models effectively account for the spatial behavior of RC slabs and slip effects while maintaining computational efficiency.

To further reduce computational demands, many researchers have adopted beam finite element models for nonlinear analyses of composite frames [11-15]. These models evaluate the flexural stiffness of composite beams using the moment-curvature (M-ϕ) relationship, derived from the constitutive stress-strain behavior of concrete and steel. The approach requires either dividing elements into multiple sub-elements with lumped plastic hinges or using a single element with spreading plastic hinges. However, despite its efficiency, this method still involves significant effort in formulating the governing equations [13,14].

Recent advancements in composite girder analysis have focused on addressing complex behaviors such as partial shear interaction, shear deformability, and time-dependent effects. Several studies [16-18] have incorporated partial shear connection and shear

deformation into finite element models to improve accuracy, particularly for cases where bending–shear interaction is significant. Zona and Ranzi [16] demonstrated that while differences between models are minimal in flexure-dominated behavior, neglecting shear effects can lead to substantial discrepancies when shear forces become influential. Similarly, Ranzi et al. [18] quantified the underestimation of deflections due to ignoring shear deformability, highlighting its impact in both simply supported and continuous girders. In addition to shear-related effects, recent research has also addressed time-dependent behaviors such as creep and shrinkage, which can significantly influence the long-term performance of composite girders [19].

By enhancing both computational efficiency and accuracy, this study advances structural analysis and design methodologies, enabling engineers to optimize composite structures with greater confidence. The proposed method, based on a force-based formulation using three-moment equations, directly relates bending moments at consecutive supports, allowing efficient analysis of continuous girders while accurately capturing nonlinear behavior such as gradual and distributed yielding. Compared to conventional displacement-based methods, which rely on approximating displacement fields and require extensive element subdivision and complex computations, the force-based approach offers superior handling of flexurally dominated nonlinearities with reduced computational effort. While displacement-based methods are widely used for their simplicity in general applications, they often struggle with accurately representing distributed plasticity without fine meshing. The proposed method overcomes these limitations, providing a practical and reliable tool with significant implications for both academic research and engineering practice.

2. RESEARCH SIGNIFICANCE

This study introduces an innovative method to develop an exact moment-curvature curve for steel-concrete composite cross-sections, offering a breakthrough in accuracy and efficiency. Unlike the traditional fiber method, this approach drastically reduces computational time, making it highly practical for engineering applications. Furthermore, the research presents a precise solution for determining girder deflection, addressing a critical challenge in structural analysis. By improving the computational efficiency and accuracy of these calculations, this study contributes to the advancement of structural design methodologies, enabling engineers to optimize composite structures with greater precision and confidence. Its findings have broad implications for both academia and industry.

3. THE PROPOSED METHOD

3.1 Cross Section

Figure 1 shows a typical cross-section of the steel-concrete composite girder. The dimensions include concrete slab width (b_s) and thickness (t_s), steel I-section height (h), flange width (b_f), flange thickness (t_f), and web thickness (t_w). The following assumptions are adopted in this study: (1) a perfect bond is assumed between the steel and concrete components, ensuring that plane sections remain plane after deformation; (2) shear deformation and torsional effects are neglected in the constitutive behavior of both steel and concrete; (3) large displacements and rotations are permitted, while strains are assumed to remain small; and (4) time-dependent effects (such as creep and shrinkage) and dynamic effects are not considered.

It is acknowledged that the assumption of a perfect bond between steel and concrete, along with the application of Euler–Bernoulli beam theory, may introduce limitations, particularly for long-span girders, partial shear connections, or cases involving high shear forces. However, for typical continuous composite girders with moderate spans and adequately designed shear connectors, these assumptions provide a reasonable balance between analytical simplicity and accuracy. Therefore, these assumptions are deemed appropriate for the scope of this study, which focuses on capturing the primary nonlinear flexural behavior. This study assumes full composite action with an adequate number of shear connectors to prevent significant slip between the steel beam and concrete slab. As such, shear deformation and connector spacing effects are not explicitly considered. This assumption is appropriate for typical design scenarios where connectors are provided in accordance with code requirements to ensure full interaction.

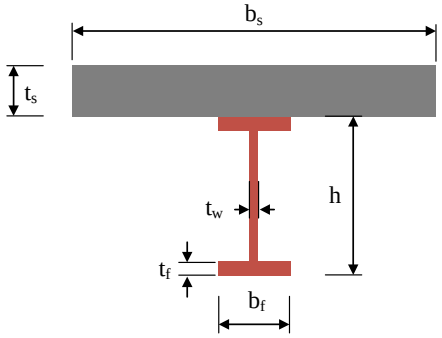

Fig. 1 Typical cross-section

3.2 The Behavior of Structural Steel

Due to the limited available parameters for steel behavior, this study adopts the simplest stress-strain

relationship. The axial stress-strain response of the structural steel material is assumed to be elastic-perfectly plastic in both tension and compression [9], without considering hardening effects, as shown in Fig. 2 and expressed in Eq. (1) below:

$$\sigma_s = \begin{cases} s\,E_s\varepsilon_s, |\varepsilon_s| \le \varepsilon_{ys} \\ s\,f_{ys}, \varepsilon_{ys} < |\varepsilon_s| \end{cases} \quad (1)$$

where σ_s is axial stress and ε_s is axial strain; $s=s(\varepsilon_s)$ is signum function of ε_s, s=1 if $\varepsilon_s \ge 0$, and s=-1 if $\varepsilon_s<0$; f_{ys} is yield strength and ε_{ys} is yield strain; E_s is Young's modulus.

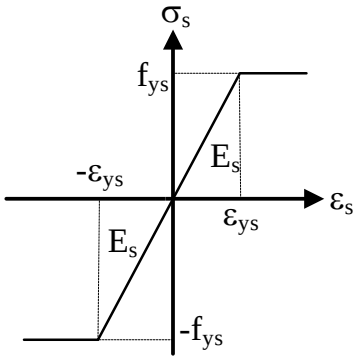

Fig. 2 The stress-strain relationship for steel

3.3 The Behavior of Concrete

The constitutive model for concrete under compression is represented by a combination of a second-degree parabola for ascending part and a straight line for descending part [20], as depicted in Fig. 3 and presented in Eq. (2):

$$\sigma_c = \begin{cases} -f_c\left[2\left(\dfrac{-\varepsilon_c}{\varepsilon_{0c}}\right)-\left(\dfrac{\varepsilon_c}{\varepsilon_{0c}}\right)^2\right], -\varepsilon_{0c} \le \varepsilon_c \le 0 \\ -f_c\left[1-(1-\eta)\dfrac{-\varepsilon_c-\varepsilon_{0c}}{\varepsilon_{uc}-\varepsilon_{0c}}\right], -\varepsilon_{uc} \le \varepsilon_c < -\varepsilon_{0c} \\ -\eta f_c, \varepsilon_c < -\varepsilon_{uc} \end{cases} \quad (2)$$

where ε_c is axial strain and σ_c is axial stress of the concrete; f_c is prism compressive strength in uniaxial loading, taken as $0.76f_{uc}$, where f_{uc} represents the cubic compressive strength and can be approximately evaluated as $1.25f_{0c}$ where f_{0c} represents the cylinder compressive strength; E_c denoted Young's modulus of the concrete, can be computed by using ACI318-08 [21] equation as $E_c = 4700\sqrt{f_c(MPa)}$ (MPa) for normal weight concrete; ε_{0c} is a corresponding strain to f_c, $\varepsilon_{uc}=2f_c/E_c$; ε_{uc} is ultimate strain; and η is residual stress factor.

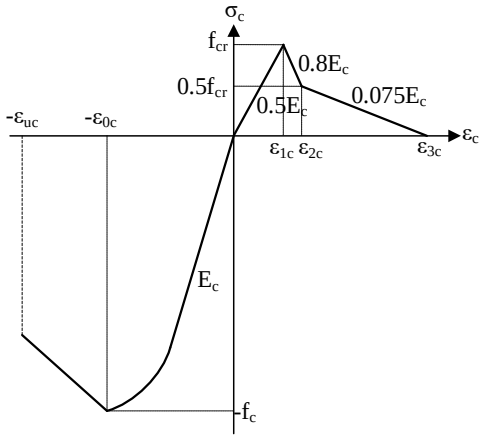

Fig. 3 The stress-strain relationship for concrete

The stress-strain relationship of concrete in tension developed by Vebo and Ghali [22] was adopted in this study, given in the following forms:

$$\sigma_c = \begin{cases} 0.5E_c\varepsilon_c,\ \varepsilon_c \le \varepsilon_{1c} \\ f_{cr} - E_{cr1}(\varepsilon_c - \varepsilon_{1c}),\ \varepsilon_{1c} < \varepsilon_c \le \varepsilon_{2c} \\ 0.5\,f_{cr} - E_{cr2}(\varepsilon_c - \varepsilon_{2c}),\ \varepsilon_{2c} < \varepsilon_c \le \varepsilon_{3c} \\ 0,\ \varepsilon_c > \varepsilon_{3c} \end{cases} \quad (3)$$

where f_{cr} represents the tensile strength of concrete; ε_{1c} is strain corresponding to cracking stress; ε_{2c} is strain corresponding to tensile stress reducing to half of cracking stress after cracking, $\varepsilon_{2c}=2.625f_{cr}/E_c$; ε_{3c} is strain corresponding to zero tensile stress; and $E_{cr1}=0.8E_c$ and $E_{cr2}=0.075E_c$ are cracking moduli. The stress-strain curve of the concrete for both compression and tension is illustrated in Fig. 3. The number inside the circle indicates the segment number that is used to establish equation of stress to determine moment-curvature curve.

3.4 The Behavior of Steel Rebar

When the steel bar is subjected to tension, the crack in concrete will lead to the inhomogeneous distribution of stress of the steel bar along the longitudinal direction. Based on experimental results and theoretical analysis, Berlabi and Hsu [23] proposed a method for considering the inhomogeneous distribution of stress and smeared crack model. An average stress-strain curve represents stress-strain relationship of the embedded rebar in tension was developed (as shown in Fig. 4) expressed in the following equation:

$$\sigma_r = \begin{cases} E_r\varepsilon_r, -\varepsilon_{yr} \le \varepsilon_r \le \varepsilon_{nr} \\ f_{yr}\beta, \varepsilon_{nr} < \varepsilon_r \le \varepsilon_{ur} \\ f_{yr}, \varepsilon_r > \varepsilon_{ur} \\ -f_{yr}, \varepsilon_r < -\varepsilon_{yr} \end{cases} \quad (4)$$

where ε_r is axial strain and σ_r is axial stress of the rebar; E_r and f_{yr} are Young's modulus and yield

strength of the rebar material, respectively; f_{nr} and ε_{nr} is the average yield stress and yield strain, respectively; ε_{ur} is the ultimate strain; and E_{hr} is hardening modulus. More details about the model can be found in Berlabi and Hsu [23].

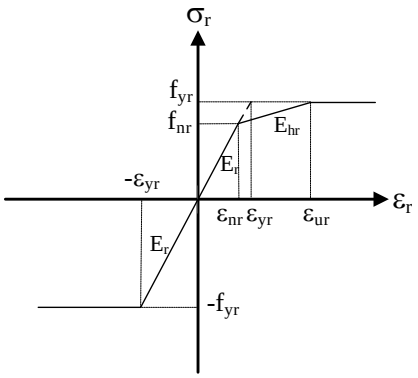

Fig. 4 The stress-strain relationship for rebar

3.5 The Proposed Method

The three-bending-moment equation based on force method and iteration method are adopted to solve the nonlinear behavior of the continuous girder. The applied loads are divided into number of load steps and the increment unknown moments at the supports can be solved linearly. The following equations for the continuous girder with N spans in Fig. 5 can be obtained [24]:

$$\begin{bmatrix} \delta_{11} & \delta_{12} & 0 & ... & 0 \\ \delta_{21} & \delta_{22} & \delta_{23} & ... & 0 \\ 0 & \delta_{23} & \delta_{33} & ... & 0 \\ ... & ... & ... & ... & ... \\ 0 & 0 & 0 & ... & \delta_{nn} \end{bmatrix} \begin{Bmatrix} \Delta M_1 \\ \Delta M_2 \\ \Delta M_3 \\ ... \\ \Delta M_n \end{Bmatrix} = \begin{Bmatrix} \delta_{1p} \\ \delta_{2p} \\ \delta_{3p} \\ ... \\ \delta_{np} \end{Bmatrix} \quad (5)$$

where:

$$\delta_{i,i} = \int_0^{L_i} \frac{1}{EI_i}\left(\frac{x}{L_i}\right)^2 dx + \int_0^{L_{i+1}} \frac{1}{EI_{i+1}}\left(\frac{L_{i+1}-x}{L_{i+1}}\right)^2 dx \quad (6a)$$

$$\delta_{i,i+1} = \int_0^{L_{i+1}} \frac{1}{EI_{i+1}}\left(\frac{x}{L_{i+1}}\right)\left(\frac{L_{i+1}-x}{L_{i+1}}\right) dx \quad (6b)$$

$$\delta_{i,p} = \int_0^{L_i} \frac{1}{EI_i}\left(\frac{x}{L_i}\right)\Delta M_{p,i}\,dx + \int_0^{L_{i+1}} \frac{1}{EI_{i+1}}\left(\frac{L_{i+1}-x}{L_{i+1}}\right)\Delta M_{p,i+1}\,dx \quad (6c)$$

where i=1÷n denoted as index of unknown internal moments at the supports, ΔM_i, and the left span length of the ith support, L_i; n=N-1; EI is tangential stiffness of the composite cross section; ΔM_p is increment bending moment in the primary system due to applied load; L is span length. The derivation of these equations follows the classical development of the three-moment equation as detailed in [24]. For completeness, a brief outline of the key steps is provided here, while full derivations can be found in the referenced work. It is important to note that the derivation of the governing equations is based on the assumption of full composite action, where a perfect bond between steel and concrete is maintained. As a result, slip effects and partial interaction behavior are not included in this formulation, allowing for a simplified yet accurate representation of the nonlinear flexural response.

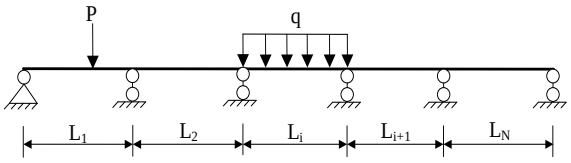

a) Geometry of the continuous girder

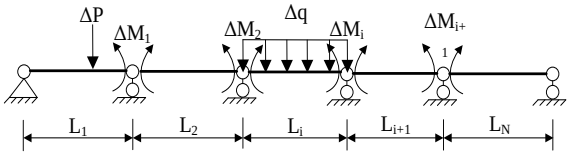

b) Internal moments of the conjugate girder

Fig. 5 The continuous girder

The internal bending moments at the ith span of the girder then computed as follows:

$$M_{x,i,j} = M_{x,i,j-1} + \frac{x}{L_i}\Delta M_i + \left(1-\frac{x}{L_i}\right)\Delta M_{i-1} + \Delta M_{p,x,i} \quad (7)$$

Based on bending moments along the girder and moment-curvature curve, the curvature along the girder can be obtained as:

$$\phi = \phi(M) \quad (8)$$

The moment-curvature curves can be obtained based on a method proposed by Hoang [25]. The rotation and displacement of the girders can then be calculated by using the following equations [26]:

$$\theta = \int \phi dx + C \qquad w = \int\int \phi dx dx + Cx + D \quad (9)$$

where C and D are constants of integrations determined from boundary conditions. Equation (8) can be implemented using the Riemann integral, which is defined as a limit of sums. This approach, as described by Bear [27], allows for the calculation of the integral by summing the contributions from each small segment of the girder and taking the limit as the segment size approaches zero. The boundary conditions are applied at both span ends by setting displacements in Eq. (9) to zero, assuming perfectly rigid supports that prevent vertical displacement and eliminate additional deformations or moment redistribution. At the first end, x=0, and the

integration $\int\int \phi dxdx = 0$, and at the second end, $x=L_i$, the constants of integrations at the ith span can be obtained as:

$$D_i = 0 \quad (10)$$

$$C_i = -\frac{1}{L_i}\int_0^{L_i}\int_0^{L_i} \phi dxdx \quad (11)$$

The algorithm of the solution method is illustrated in Fig. 6. It should be noted that the proposed method employs an explicit iteration scheme, where tangential stiffness is updated based on the curvature from the previous step, thus eliminating the need for a conventional convergence criterion.

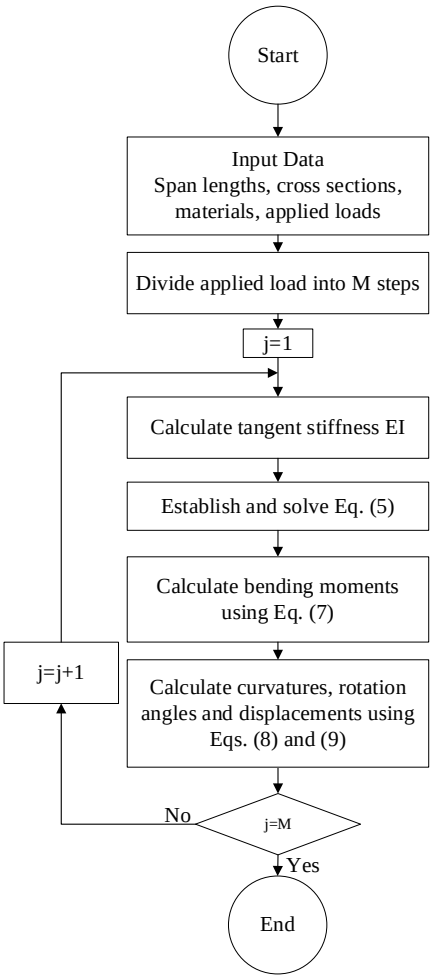

Fig. 6 Solution flow chart

4. EXAMPLES AND DISCUSSIONS

4.1 Two-Span Continuous Composite Girder Tested By Ansourian [28]

The specimen CTB4, from a series of continuous composite beams tested by Ansourian [28], is selected for analysis in this study to verify the accuracy of the proposed method. The beam was subjected to two vertical concentrated loads at the middle of each span, as shown in Fig. 7a. It consists of a concrete slab measuring 0.1 m × 0.8 m and an IBPL200 steel section, with dimensions illustrated in Fig. 7b. The concrete slab had a compressive strength of 34 MPa, a tensile strength of f_{cr}=3.6 MPa, and a Young's modulus of E_c=27,406 MPa, both calculated based on ACI318-08 [21] equations described above. The moment-curvature curve developed for this composite cross section is depeicted in Fig. 8.

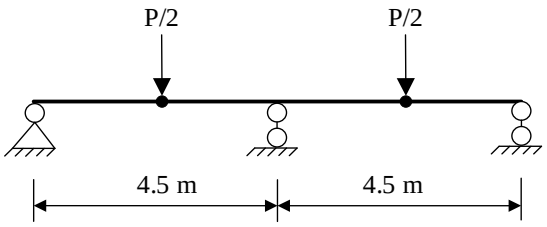

a) Geometry

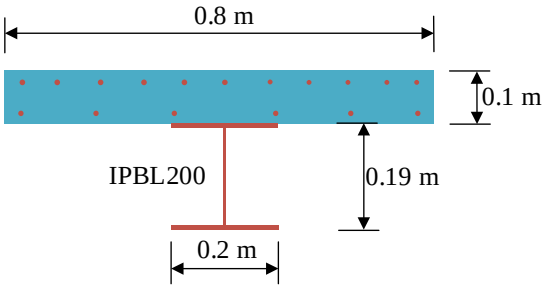

b) Cross section

Fig. 7 The model test by Ansourian [28]

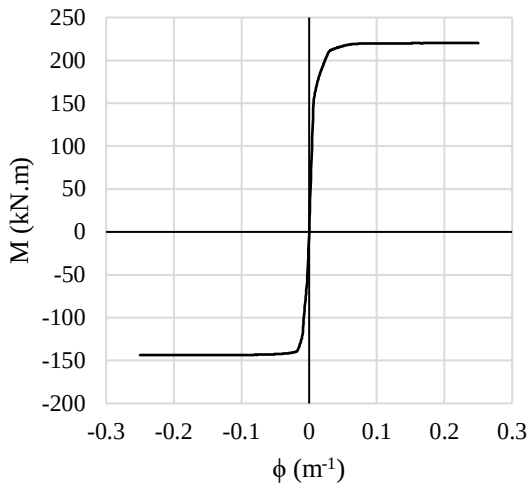

Fig. 8 M-ϕ curve for the model test by Ansourian [28]

Figure 9 presents a comparison of the results obtained from the proposed method, experimental data, and the theoretical model by Ansourian [28]. The load-displacement curve from the proposed method closely aligns with the theoretical curve; however, both tend to overestimate the load-displacement relationship compared to the experimental results. This discrepancy arises from not accounting for shear slip between the concrete slab and the steel section. Nevertheless, the proposed

method accurately predicts the girder capacity at P = 520 kN, which is very close to the experimental girder capacity of P = 518 kN.

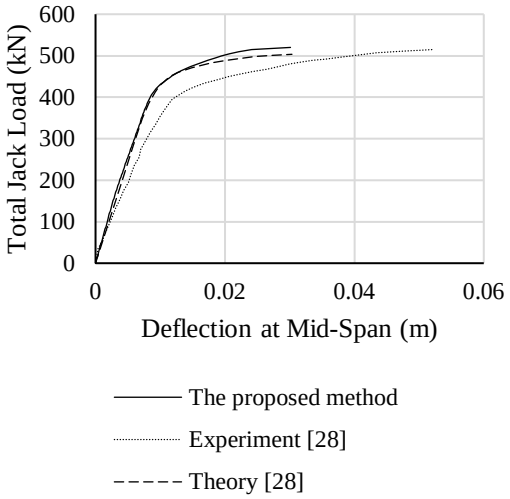

Fig. 9 Load-displacement curves at mid-span for the model test by Ansourian [28]

4.2 Two-Span Continuous Composite Girder Tested By Slutter and Driscoll [29]

The two-span continuous composite girder was tested by Slutter and Driscoll [29] and numerically analyzed by Nie et al. [9] and Chiorean [14]. The geometry with applied load locations and section properties of the girder are depicted in Fig. 10. The concrete in compression had a cylinder compressive strength of f'_c = 16 MPa, while the structural steel had a yield stress of f_{sy} = 252.4 MPa and a Young's modulus of E_s = 20,000 MPa.

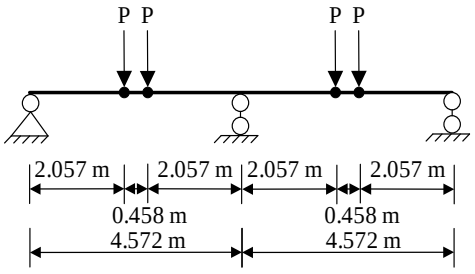

a) Geometry

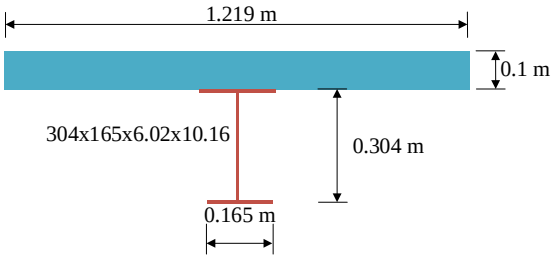

b) Cross section

Fig. 10 The model test by Slutter and Driscoll [29]

As shown in Fig. 12, the behavior of the continuous composite girder predicted by the present analysis closely aligns with both the experimental test results [29] and the mixed finite element analysis [9], accurately capturing the girder's capacity.

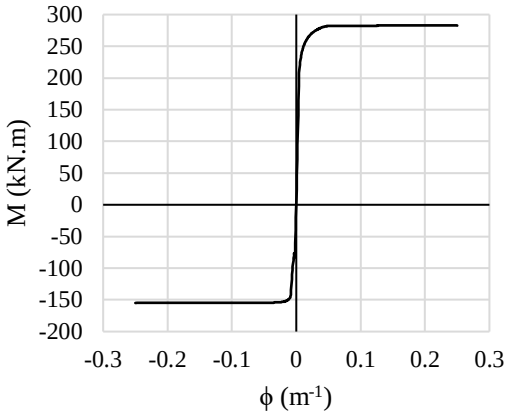

Fig. 11 M-ϕ curve for the model test by Slutter and Driscoll [29]

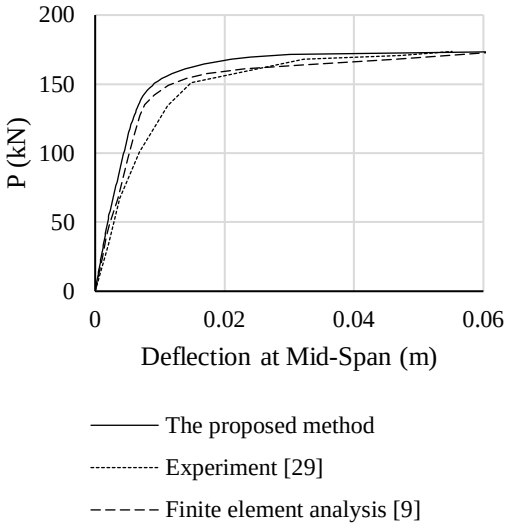

Fig. 12 Load-displacement curves for the model test by Slutter and Driscoll [29]

4.3 Two-Span Continuous Composite Girder Tested By Yam and Chapman [30]

The continuous beam had two equal spans of 3.55 m each (Fig. 13a) and consisted of a 0.152 m deep I-section with a yield strength of 270 MPa. The steel girder was connected to a 0.06 m thick, 0.92 m wide concrete slab using stud shear connectors. The compressive strength of the slab is 47.6 MPa. More details of the cross section of the girder is shown in Fig. 13b. The moment-curvature curve, shown in Fig. 14, reveals a softening range on the negative side of the curvature, indicating concrete cracking behavior. The proposed solution also captures the negative tangent stiffness of the cross-section.

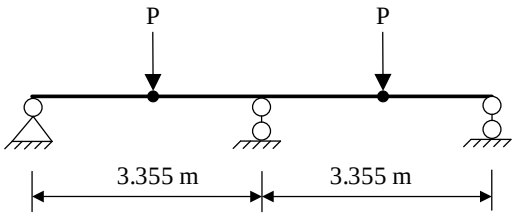

a) Geometry

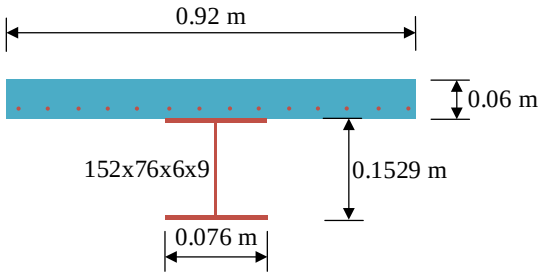

b) Cross section

Fig. 13 The model test by Yam and Chapman [30]

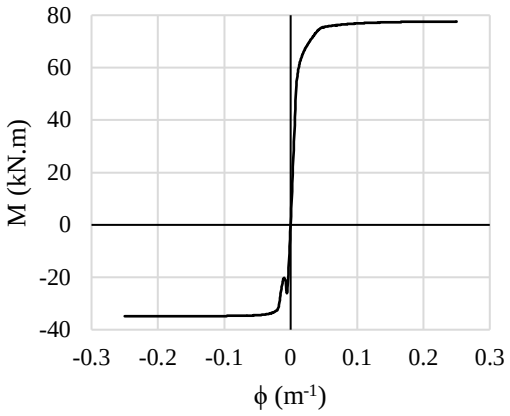

Fig. 14 M-ϕ curve for the model test by Yam and Chapman [30]

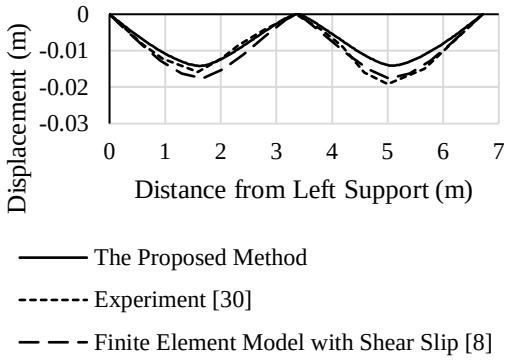

Fig. 15 The model test by Yam and Chapman [30]

Due to the absence of a load-displacement curve, the comparison is made using the deflection curve of the entire girder at P=108.5 kN, which is considered the maximum applied load. Razaqpur and Nofal [8] conducted finite element analyses using shell elements and material models capable of capturing the shear effect between the concrete slab and the steel section. As the proposed method does not account for shear effects, the predicted deflection curve underestimates by 11% compared to Razaqpur and Nofal [8], and by 20% compared to the experimental results of Yam and Chapman [30].

5. CONCLUSIONS

This study presents a simple yet highly accurate analytical solution for analyzing the nonlinear behavior of continuous steel-concrete composite girders. The key conclusions drawn from this research are as follows:

- For the first time, the three-moment equation based on the force method is applied to the nonlinear analysis of continuous girders, effectively capturing gradual and distributed yielding.
- The proposed method produces results that closely align with those obtained from the mixed finite element method and the plastic hinge method.
- The comparisons with three full-scale test results from the literature with either acceptable discrepancies or high accuracy in predicting girder capacities, confirming the robustness of the proposed method.

The proposed analytical method offers practicing engineers a straightforward and reliable tool for assessing the nonlinear flexural behavior of continuous steel-concrete composite girders. By eliminating the need for complex finite element modeling while maintaining high accuracy, this method supports efficient design verification and performance evaluation in typical engineering applications. Future work may extend the proposed method by incorporating shear slip effects and shear deformation, enabling its application to composite girders with partial shear connection or cases where shear-lag significantly influences global behavior, and accounting for cyclic or fatigue loading.

6. REFERENCES

[1] Mahmoud A, Najjar S. S., Mabsout M. and Tarhini K. M., Reliability analysis of reinforced concrete slab bridges, International Journal of GEOMATE, 13(36), 2017, pp.44-49.

[2] Apriani W., Suryanita R., Firzal Y. and Lubis F., Damage prediction of the steel arch bridge model based on artificial neural network method. International Journal of GEOMATE, 20(82), 2021, pp.46-52.

[3] He J., Li C., Liu Y. and Chen A., Performance of steel I-girder strengthened by concrete encasement under hogging moment. In Proceedings of the fourth international symposium on life-cycle civil engineering 2015.

[4] Vasdravellis G., Uy B., Tan E.L. and Kirkland B., Behaviour and design of composite beams subjected to negative bending and compression. Journal of Constructional Steel Research, 79, 2012, pp.34-47.
[5] Lin W., Experimental investigation on composite beams under combined negative bending and torsional moments. Advances in Structural Engineering, 24(7), 2021, pp.1456-65.
[6] Wegmuller A. W. and Amer H. N., Nonlinear response of composite steel-concrete bridges. Computers & Structures, 7(2), 1977, pp.161-9.
[7] Hirst M. J. and Yeo M. F., The analysis of composite beams using standard finite element programs. Computers & Structures, 11(3), 1980, pp.233-7.
[8] Razaqpur A. G. and Nofal M., A finite element for modeling the nonlinear behavior of shear connectors in composite structures. Journal of Computers and Structures, 32(1), 1989, pp.169-174.
[9] Nie J., Tao M., Cai C. S. and Chen G., Modeling and investigation of elasto-plastic behavior of steel-concrete composite frame systems. Journal of Constructional Steel Research, 67(12), 2011, pp.1973-1984.
[10] Zhou F., Mosalam K. M. and Nakashima M., Finite-element analysis of a composite frame under large lateral cyclic loading. Journal of Structural Engineering, 133(7), 2007, pp1018-26.
[11] Deng L. and Ghosn M., Nonlinear analysis of composite steel girder bridges. Engineering Journal, 37(4), 2000, pp.140-156.
[12] Jiang X. M., Chen H. and Liew J. Y. R., Spread of plasticity analysis of three-dimensional steel frames. Journal of Constructional Steel Research, 58, 2002, pp.193-212.
[13] Iu C. K., Bradford M. A. and Chen W. F., Second-order inelastic analysis of composite framed structures based on the refined plastic hinge method. Engineering Structures, 31(3), 2009, pp.799-813.
[14] Chiorean C. G., A computer method for nonlinear inelastic analysis of 3D composite steel-concrete frame structures. Engineering Structures, 57, 2013, pp.125-152.
[15] Ravi Mullapudi T. and Ayoub A., Fiber beam analysis of reinforced concrete members with cyclic constitutive and material laws. International Journal of Concrete Structures and Materials, 12(1), 2018, pp.1-16.
[16] Zona A. and Ranzi G., Finite element models for nonlinear analysis of steel–concrete composite beams with partial interaction in combined bending and shear. Finite Elements in Analysis and Design, 47(2), 2011, pp.98-118.
[17] Chiorean C. G. and Buru S. M., Practical nonlinear inelastic analysis method of composite steel-concrete beams with partial composite action. Engineering Structures, 134, 2017, pp.74-106.
[18] Ranzi G., Leoni G. and Zandonini, R., State of the art on the time-dependent behaviour of composite steel–concrete structures. Journal of constructional steel Research, 80, 2013, pp.252-263.
[19] Zhao G. Y., Liu W., Su R. and Zhao J. C., A beam finite element model considering the slip, shear lag, and time-dependent effects of steel–concrete composite box beams. Buildings, 13(1), 2023, pp.215-236.
[20] Kent D. C. and Park R., Flexural Members with Confined Concrete. Journal of the Structural Division ASCE, 97(ST7), 1971, pp.1969-1990.
[21] ACI Committee, Building code requirements for structural concrete and commentary. In American Concrete Institute, 2008, pp.1-471.
[22] Vebo A. and Ghali A., Moment-Curvature Relations of Reinforced Concrete Slab. J Struct Div ASCE, 103(ST3), 1977, pp.515–531.
[23] Belarbi A. and Hsu T. T., Constitutive laws of concrete in tension and reinforcing bars stiffened by concrete. Structural Journal, 91(4), 1994, pp.465-474.
[24] Hibbeler R. C., Structural Analysis, Boston, Prentice Hall, 1999, pp.378-383
[25] Hoang N. H., Plastic analysis of concrete-steel frame under static load. Dissertation, Hanoi Architectural University (in Vietnamese), 2020, pp.1-178.
[26] Hoang N. H., Vu A. Q. and Nghiem H. M., Analytical solution for the nonlinear behavior of steel-concrete composite girders.. International Journal of GEOMATE, 28(128), 2025, pp.1-8.
[27] Bear H. S., A primer of Lebesgue integration. Academic Press 2002, pp.1-164.
[28] Ansourian P., Experiments on continuous composite beams. Proceedings of the Institution of Civil Engineers,71(2), 1981, pp.25-71.
[29] Slutter R. G. and Driscoll G. C., Flexural strength of steel–concrete composite beams. Journal of the Structural Division ASCE, 91, 1965, pp.71-99.
[30] Yam L. C. P. and Chapman J. C., The inelastic behavior of continuous composite beams of steel and concrete. Institution of Civil Engineering, Pt2, Research & Theory, 53(12), 1972, pp487-501.